Carbon nanotubes and graphene-based chemical sensors

Abha Misra*

Department of Instrumentation and Applied Physics, Indian Institute of Science, Bangalore 560 012, India

The chemical sensing behaviour of the carbon nanotube and graphene-based sensors for detecting various chemical analytes is presented in this article. A focus on detection mechanisms has been provided to assess their relative potential under different environmental conditions. The performance of these two carbon allotropes is compared based on their sensitivity towards various types of electron donating and accepting molecules. Although these carbon materials still have to meet crucial challenges in fabrication and optimization, continued progress in this field may lead to a sensor with superior sensitivity for a wide range of applications.

Keywords: Carbon nanotubes, chemical sensors, electron donors and acceptors, graphene.

Introduction

CARBON-BASED technology has been emerged to develop highly sensitive, inexpensive and low-power devices proposing an alternative to silicon-based conventional technology that involves rigorous fabrication steps using top-down approach. Also, it has already been speculated that the scaling of silicon-based devices will soon reach their limit[1]; therefore, there is an urgent need to explore novel materials. Carbon materials such as carbon nanotubes (CNT) and graphene with inherent nanoscale characteristics have offered a great potential for presenting next-generation material for diverse applications such as field emission, electronics, sensors and energy[2–9]. High quality crystal lattices provide these materials excellent carrier mobility (e.g. ballistic conduction) with much lower thermal and electrical noises[8,9]. In addition, multifunctional characteristics such as high mechanical strength, high thermal conduction and selective optical properties presented their applicability in various interdisciplinary research fields. The high electrical conductivity and optical transparency also suggest both the materials as candidates for transparent conducting devices, specially required in touch-screens, liquid crystal displays, organic photovoltaic cells and organic light-emitting diodes[8,10–18]. Moreover, being single-crystal materials, both provide an easy understanding about the working mechanism as well as control over engineering their functionalities, which can easily be modelled using computational techniques.

The significance of these materials arises due to a need to address the following key issues such as self-contained integrated device without any size constraint, being able to modify and design favourable interfaces to attract chemical analytes, achievement of efficient transduction for enhancing sensitivity and selectivity of the chemicals and faster response time in very sensitive systems. Low-dimensional materials have shown potential to majorly solve these issues because materials at this dimension provide an important surface chemistry than in bulk, and the role of CNT and graphene has become important due to their tunable characteristics. This review focuses on the specific properties of these materials, which contribute to solving the above-mentioned issues for chemical sensing. Both graphene and CNT have emerged as materials having exceptional electronic, mechanical, thermal and optical properties due to unique one- and two-dimensional sp^2-bonded structure respectively. While both show a high sensitivity towards any changes in their chemical environment, the advantages in structural properties make one material favourable over the other. CNT have high aspect ratios, while graphene has greatest possible surface area per unit volume to adsorb chemical species. Therefore, the present article will highlight the relevant properties of both CNT and graphene in the context of chemical sensing, which will elucidate the fundamental differences in the working principle of chemical sensors.

The detection efficiency of the chemical sensor is significantly important to accurately monitor the concentration of various toxic gases in the atmosphere. Ammonia (NH_3) and nitrogen dioxide (NO_2) adversely affect human health and pollute the environment, and sources of these gases are primarily agriculture, natural waste products, industrial products as well as manufacturing of chemicals. Moreover, presence of high concentrations of hydrogen (H_2) and methane (CH_4) becomes explosives. Therefore, including these and all other gases and vapours (SO_2, H_2S, NO, CO_2, EtOH, etc.) which adversely impact our environment and safety, high-precision detection has become important. This article aims at presenting an overview on CNT and graphene-based new-generation

*e-mail: abha@isu.iisc.ernet.in

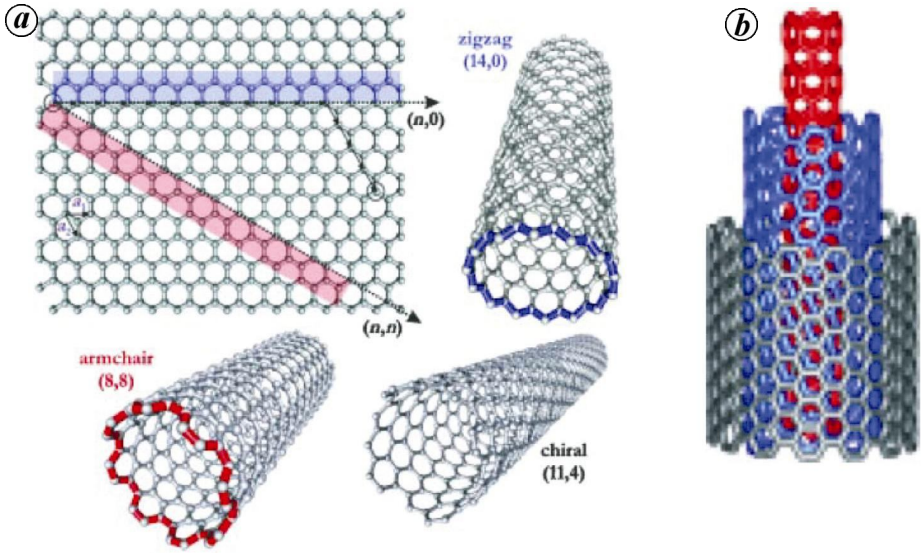

Figure 1. ***a***, Schematic demonstration of the roll-up graphene to form zigzag, armchair and chiral CNT. Chiral vectors are shown in the respective directions. ***b***, Computational image of a MWCNT consisting of concentric graphene walls[2].

chemical sensors. The motivation in selecting this topic lies in developing an understanding of the working principle of these two materials, which can answer the following questions: what specific advantages do CNT and graphene provide over conventional materials for chemical sensing of gases and vapours. Which of these two materials provide significant advantages for the detection, and how can we improve the development of these sensors to expedite the current technology.

Properties of carbon nanotubes

Single-walled carbon nanotubes (SWCNT) and multi-walled carbon nanotubes (MWCNT) have single and several concentric tubes respectively, with a common axis along the length of the individual CNT. Higher aspect ratio between the tube length and diameter provides an important characteristic to CNT to utilize them for large-scale applications. Importantly, CNT are electrochemically active due to the asymmetrical distribution of electron clouds around them, which provide a rich π-electron conjugation along the CNT walls[19]. Furthermore, electronic properties of SWCNT are controlled by its rolling direction, which is known as chirality (Figure 1).

It is the angle of rolling of graphene sheet that provides alignment of π-orbitals. The chiral vector $\vec{C} = n\vec{a}_1 + m\vec{a}_2$, where ($n$, m) are integers of hexagons, can be obtained after traversing in the two-unit vector directions a_1 and a_2 in the planar lattice of graphene. These vectors help in determining electrical properties of the resulting SWCNT; if ($n - m$) is a multiple of 3, then the resulting CNT will be metallic, otherwise it will be semiconducting in nature[2].

Large-scale synthesis of carbon nanotubes

CNT are synthesized by employing various techniques such as arc discharge, laser abalation or chemical vapour deposition (CVD). Using arc discharge, the yield is up to 30% by weight[20]; however, laser ablation produces about 70% by vapourizing a graphite target in a high-temperature reactor. The catalytic vapour deposition of CNT at 700–800°C gives the highest yield. This is the most common method for commercial production. In this process the substrate is heated to high temperature in the presence of a process gas and carbon-containing gases. CNT grow at the catalyst metal sites. Carbon-containing gas breaks at the surface of the catalyst particles. Then carbon is transported to the edge of the deposited particles on the substrate, where CNT form. Then catalyst particles can stay at the tip or base of the CNT. Also, if the plasma is created by electric field during the growth process (plasma-enhanced chemical vapour deposition), then the CNT growth follows the direction of the applied electric field. However, without plasma CNT randomly align on the substrate. Overall, for CNT synthesis laser ablation is the most expensive and arc discharge results in a low yield. Therefore, CVD is the most promising method for industrial-scale deposition. The length of CVD-grown CNT can be varied from microns to millimetres.

Chemical functionalization of carbon nanotubes for gas-specific sensing

Recently, CNT-based electronic gas sensors either in the form of chemiresistors or back-gated field-effect transistors have been designed to detect various gases. In these sensors, CNT are often used after doping or

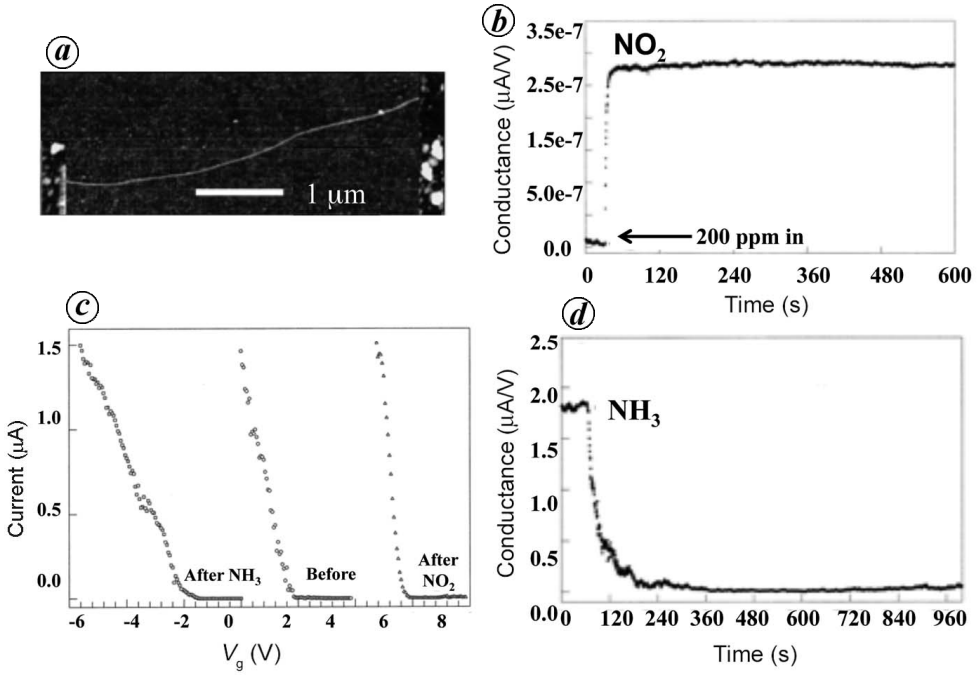

Figure 2. ***a***, Atomic force microscopic image of the semiconducting SWCNT between metal electrodes, used as sensor device. ***b***, Current response of SWCNT-based FET device with the gate voltage ($I - V_g$) measured for both NO_2 and NH_3 gases. ***c***, ***d***, Conductance versus time response for 200 ppm NO_2 and 1% NH_3 exposures respectively[5].

functionalization with different polymers[21–24] and metal/metal oxides[25–28] to enhance the selective detection to different gases and the sensitivity of CNT-based sensors. Generally, CNT accept electrons in the sensing process; hence hole density in the defect sites decreases, which reduces the current. The response time of CNT is mainly governed by the generation of the charge carriers in the defect sites and depends on how quickly these carriers can be transported from the defect sites to the electrodes. This section provides details on chemical modification of CNT for various gases.

Carbon monoxide (CO) is an odourless and colourless gas. The primary constituent of coal gas is widely used for domestic cooking/heating. CO combines with a haemoglobin to form carboxyhaemoglobin, which obstructs oxygen transportation in the body. High concentration (> 150 ppm) of CO becomes a health hazard and even leads to death. Hence due to its toxicity, it is important to sense even traces of CO. CNT are used for CO sensing using several methods of functionalization. Zhao *et al.*[29] demonstrated high selectivity in oxygen plasma-modified CNT that can be used effectively for CO sensing up to 5 ppm at room temperature. The main reason for this detection was stated through generation of disorder structures that led more gas molecules to be adsorbed, as described earlier. Dong *et al.*[30] used carboxylic acid-functionalized CNT for detection of 10 ppm CO gas through weak hydrogen bonding with the attached carboxylic group. Thus, the carboxylic acid group was shown to play a key role in CO gas detection, when a decrease in the electrical resistance of CNT was observed, despite CO being an electron-withdrawing gas. Carbon dioxide is a reducing gas and its absorption in CNT takes place through injection of electrons. In *p*-type semiconductor, holes are the main charge carriers and depletion of holes will result in an increase in resistivity or decrease in conductivity of the material. Ong *et al.*[31] demonstrated MWCNT composite with SiO_2 for CO_2 detection on a planar inductor–capacitor resonant circuit. CNT functionalized with a polymer matrix consisting of polyethylenimine (PEI) and starch showed excellent sensitivity up to 500 ppm and 10% in air. The detection of nitric oxide is important in medicine to check NO level in a patient's breath. Metal nanoparticles (Pt, Pd, Au, Ag) decorated CNT show a unique electrical response to NO detection[32], whereas WO_3 films impregnated with CNT show sensitivity to 500 ppb under ambient condition. Ammonia and nitrogen dioxide gases have also been detected using polymer poly(*m*-aminobenzene sulphonic acid) (PABS) and polymer polyaniline (PANI).

Carbon nanotube-based chemical sensors

It is important to recognize the nature of CNT for operation of CNT-based field-effect transistors (FET). Kong *et al.*[5] fabricated the first CNT gas sensor in 2000. Thereafter, several efforts have been made to improve the

performance of CNT gas sensors, which includes polymer functionalization, metal nanoparticle decoration, etc.[33–36]. The underlying sensing mechanism still remains unclear despite the tremendous progress made. Majority of the sensors involve changes in their electrical conductivity due to the local chemical environment. For example, interaction with electron-donating species will result into lower holes concentration, which shifts transfer characteristic towards negative voltages, while electron withdrawal will increase the holes concentration in CNT to enhance the conductance and transfer characteristic shifts towards the positive voltage side[37]. This basic approach of detecting various harmful chemicals such as NH_3, NO_2, CO, CO_2, H_2S, SO_2, etc. brings a diverse interaction mechanism, which has to be realized for better functioning of the chemical sensors. Different gases have different kinds of interactions with CNT and hence impacts on its conductivity. As mentioned earlier, the magnitude of conductivity and the positive and negative shifts with respect to the applied bias voltage provide an indication about the interacting species whether it is an electron acceptor, for example, NO_2, or an electron donor, for example, NH_3 or CO. Commercially available solid-state sensors that usually operate at high temperature show incapability for high analyte selectivity. Kong *et al.*[5] demonstrated the potential of CNT-based gas sensors (Figure 2 *a*) for NO_2 and NH_3 gases. Both NH_3 and NO_2 exposure of the semiconducting SWCNT-based sensor resulted in a shift in the transfer characteristic of approximately + 4 V and –4 V respectively (Figure 2 *b*). In addition, NH_3 exposure reduces the device current at a zero gate voltage and NO_2 increases the current at + 4 V gate voltage. The response time for detection of 200 ppm NO_2 was a few seconds (Figure 2 *c*) and for detecting 1% NH_3 it was a few minutes (Figure 2 *d*). The effect of NO_2 was explained on the basis of its electron accepting nature; it removes electrons from SWNT at a rate of approximately 0.1 electrons per NO_2 molecule upon adsorption. However, in the article of Kong *et al.*[5], the device response towards NH_3 was unclear and the authors indicated that due to lack of binding energy between gas molecule and SWCNT, NH_3 might influence indirectly the electronic properties of SWCNT.

An enhancement of NH_3 gas sensitivity at room temperature was reported by coating Co nanoparticles onto MWCNT surfaces[38]. The response was enhanced twice compared to the uncoated MWCNT and the response time for detection of 7 ppm NH_3 was 30 sec only. The response of the sensors was shown to increase more rapidly in lower concentration region compared to higher concentration region. However, the exact mechanism has not been explored. Sensitivity of the CNT-based sensor for NO_2 gas detection was further enhanced to ppb level (100–50 ppb), when Lee *et al.*[39] demonstrated the effect of both contact metals, Pt used for electrodes as well as decorated Pd nanoparticles, as shown in Figure 3 *a* and *b* respectively. The sensing response was shown to depend on the applied bias, which was explained by the formation of Schottky junction between CNT and Pt electrode, where the work functions are 4.5 and 5.65 eV respectively.

Therefore, there is an in-built potential of 1.15 eV for electrons transferring from CNT to metal electrodes (Figure 4 *a*). This potential barrier reduces under application of bias, hence carrier transfer from CNT to Pt also increases.

When Pd nanoparticles were coated onto CNT, each nanoparticle form an Schottky contact induced depletion region, which reduces the hole carrier mobility. In this case, supply of electron carriers increases electron–hole recombination by reacting with oxidizing NO_2 gas, which lowers hole carrier density in CNT, causing formation of localized depletion region. Therefore, this reaction causes an increase in the sensor resistance, thus enhancing the sensor response (Figure 4 *b*). Moreover, Lee *et al.*[39] have proposed that the arrangement of metal decoration has an advantage of preventing modification of Schottky barrier modulation by absorbed gases to ensure the sensor response is due to CNT activity only. Han *et al.*[40] demonstrated an enhanced nonlinear sensitivity in CNT and graphene oxide hybrid flexible film for NO_2 detection up to 0.5–10 ppm. This nonlinear sensitivity is due to the non-uniform diffusion of the molecules from top to bottom of the vertical CNT arrays. Further, Chen *et al.*[41] achieved a detection limit of parts per quadrillion of both NH_3 and NO_2 by *in situ* ultraviolet illumination at room temperature for removing desorbed contaminants onto the CNT surface.

CNT sensors have also been used for detecting SO_2 and H_2S, which are flammable and toxic with a lower explosive limit. SO_2 showed a similar response towards CNT as was observed for NO_2 sensing due to SO_2 being both oxidizing and reducing in nature. Zhang *et al.*[42] revealed the selectivity of MWCNT towards H_2S and SO_2 by modifying CNT with atmospheric pressure dielectric barrier discharge air plasma at different exposure times. The modified MWCNT were shown to possess a higher sensitivity towards H_2S, while they showed almost no sensitivity to SO_2. This was described as follows: plasma treatment in this study modifies the MWCNT surface by introducing carboxyl and nitrogen containing groups, therefore, under SO_2 exposure, electrons transfer from SO_2 to MWCNT takes place due to weak carboxyl oxidizability. Also, electron transfer from MWCNT to SO_2 takes place because of the presence of N atoms, which are electron-rich. When both the processes achieve equilibrium, no electron transfer takes place between SO_2 and MWCNT, which shows no sensitivity to SO_2. However, presence of carboxyl groups provides more adsorption sites for H_2S molecules and hence, there is more transfer of charges from H_2S to MWCNT.

Similarly, other gases like CO and CO_2, which are considered explosive and toxic at lower concentration

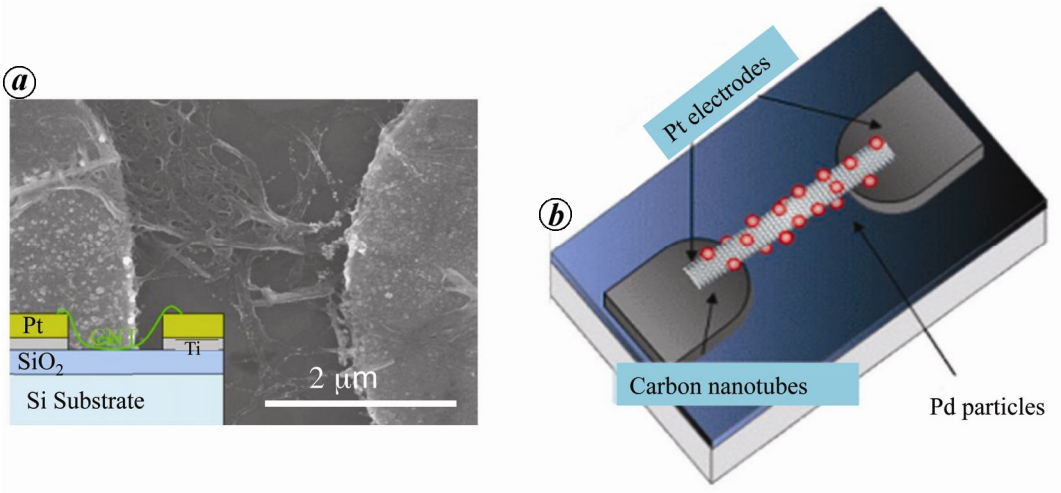

Figure 3. ***a***, Scanning electron photomicrograph of CNT on Pt electrodes. ***b***, Pd-coated CNT sensor[39].

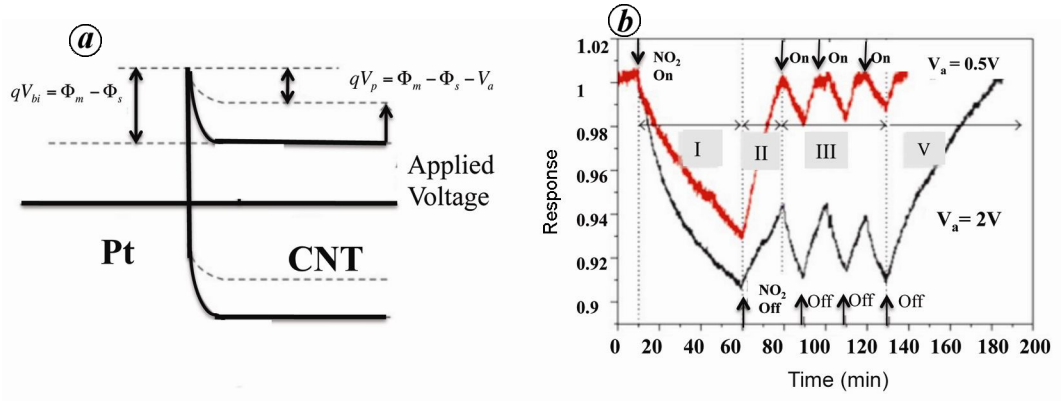

Figure 4. ***a***, Energy band structure of the junction between CNT and Pt. ***b***, Resistance change response towards NO_2 versus time at two different voltages[39].

(5–12%) in air, are also important to be detected with high precision. CNT-based sensors have played an important role for their early detection. CO absorbs onto CNT surface by hydrogen bonding through hydroxyl group formed as a result of purification process. Varghese *et al.*[43] showed that CNT could detect the presence CO through capacitive changes. Chopra *et al.*[44] detected CO in the ppb regime by changes in resonance frequency of the sensor, where gas absorption results into modifying dielectric constant of the substrate. Further, CNT functionalization with polyaniline results in a reversible response to CO for 100–500 ppm detection. Zhao *et al.*[45] have calculated a net transfer of 0.015 electrons into the CNT per adsorbing CO_2 molecule, which has not been realized experimentally so far. Moreover, excellent sensitivity to CO_2 was shown in functionalized CNT with polymer matrix consisting of PEI and starch. The response of CO_2 exposure was revealed to be reversibly decreasing, which was scaled linearly with CO_2 concentration. Ong and Grimes[31] used a composite of MWCNT and SiO_2 deposited onto planar inductor–capacitor resonant circuit. Change in resonant frequency of the sensor provided the complex permittivity of the material and the permittivity of MWCNT was shown to change linearly with CO_2 exposure.

Properties of graphene

As mentioned above, CNT have shown a great potential for chemical sensing due to excellent electrical properties, high surface to volume ratio and large gas absorption capacity. However, graphene having large specific surface area (2630 $m^2\ g^{-1}$) providing the largest sensing area per unit volume and high electron mobility at room temperature showed higher sensitivity than CNT[46]. In 1946, the electronic structure of graphene was described as a building block of the graphite. The valence and conduction bands of graphene touch at the high symmetry points K and K' of the Brilluoin zone, as depicted in Figure 5.

The interaction between graphene and the adsorbing molecule varies between weak van der Walls and strong covalent bonding, which can be readily monitored through changes in its electronic system and shows capability to detect small changes in conductivity[8]. Graphene device also showed a relatively low Johnson noise and $1/f$ noise due to high conductivity and low crystal defect density[7]. Therefore, graphene has been presented as a potential building block for next-generation high-speed and sensitive electronic devices[46–55]. This ultrahigh sensitivity of the pristine graphene is attributed to an exceptionally low-noise material.

Synthesis of graphene

There are different methods reported in the literature to fabricate graphene. Among these, mechanical cleaving of graphite, chemical cleaving or exfoliation of graphite, epitaxial growth and CVD are most widely used methods. For mechanical cleaving of graphite, a repeated stripping of graphite with adhesive tape is involved to obtain a single layer. These isolated layers can be resolved using optical microscope, atomic force microscopy or Raman spectroscopy. Chemical exfoliation of graphite employs a strong acidic solution to introduce oxygen into graphene interlayers and form graphene oxide (GO). GO can be easily separated into single layers after dispersion into an aqueous solution. Heating of hexagonal silicon carbide crystals to a high temperature (~ 1200°C) is required for epitaxial graphene by evaporating silicon and forming basal planes of graphene. A large-area graphene can be fabricated using this method. In addition, CVD allows graphene growth on metal substrates like copper and nickel using hydrocarbon gases at 700–1000°C. This method also produces a large-area graphene. However, we do not have any control over monitoring the number of layers or impurities arising during growth.

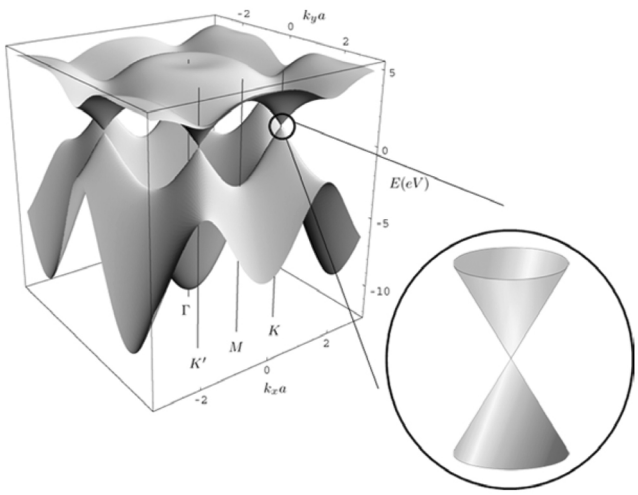

Figure 5. Band structure of graphene single layer. A linear dispersion relation is shown at the Dirac point[47].

Graphene-based sensors

Similar to CNT-based devices, graphene also presents sensitivity towards detecting adsorbed molecules onto the surface (e.g. NH_3, NO_2, CO, H_2S, NO_2, etc.). Based on different compositions and structures of the gaseous analytes, graphene interacts in distinct modes. There are several reports on revealing the strength and nature of adsorption as well as charge transfer between adsorbed analyte and graphene. Since graphene is capable of detecting individual molecule[7], it has become important to understand the charge transfer mechanism and nature of molecule–graphene interaction.

Gate voltage sweep allows following the time evolution of the Dirac peak (peak in the drain-source resistance), which emerges from the change in Fermi level in graphene due to adsorption and desorption of molecules. An approximate relationship between the number of electrons per unit area (n) and gate voltage (V_g) is used to describe the graphene response to gate voltage[56]

$$n \approx \varepsilon\varepsilon_0(V_g - V_{Dirac})/le \equiv \alpha(V_g - V_{Dirac}),$$

where $\varepsilon\varepsilon_0$ and l are the gate dielectric permittivity and thickness respectively, e is the charge of the electron and V_{Dirac} is a constant. Also, an approximate relationship between E_f and V_{Dirac} for graphene FET is given by the following equation[56]

$$E_F \approx \pm 31.7(meV/\sqrt{V})\sqrt{V_{Dirac}},$$

where e is the charge of the electron, m the mass of electron and V_{Dirac} is a constant related to the net change on the graphene. Positive and negative signs are for hole and electron conduction respectively. Romero *et al.*[56] showed a negative shift in the Dirac peaks in FET device resulting from upshifting of E_f at the Brillouin zone corners during NH_3 detection. Similar to the charge transfer of 0.03 electrons per adsorbed NH_3 molecule from NH_3 to SWCNTs (defect free), with graphene, NH_3 molecules act as donors with the same charge transfer of ~ 0.03

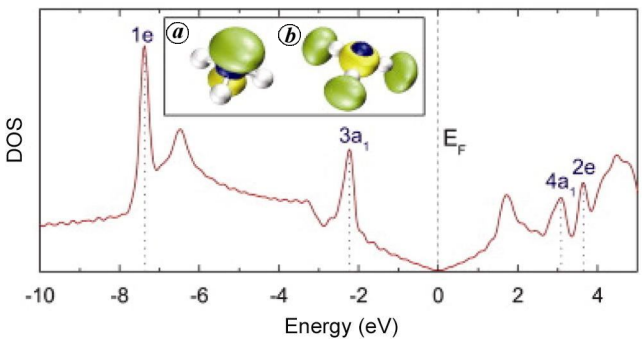

Figure 6. DOS of graphene with adsorbed NH_3 molecule. (Inset) HOMO (***a***) and LUMO (***b***) of NH_3 (ref. 57).

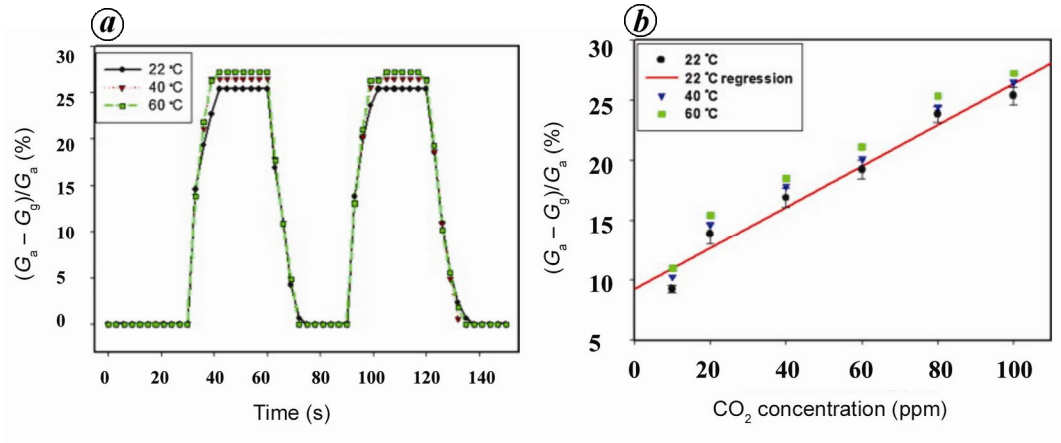

Figure 7. ***a***, Change in conductivity response of the graphene sensor with time of exposure of 100 ppm CO_2 at different temperatures. ***b***, Change in conductivity with different concentrations of CO_2 exposure[58].

electrons. In a first principle calculations, Leenaerts *et al.*[57] presented two main mechanisms for charge transfer, which depends on the magnetic properties of the adsorbing molecules. Ammonia is shown to have closed shell structure and hence is nonmagnetic, whereas NO_2 is paramagnetic when interacting with graphene monolayer. The charge transfer was shown to determine the orientation of the molecule; for example, NH_3 has shown two possible orientations w.r.t. graphene surface, one with H atoms away from the surface (*u*) and another with the H atoms pointing inside the surface (*d*), as shown in Figure 6.

A small charge transfer of 0.03 electrons was determined in the *u* direction, while there was no charge transfer in the *d* direction. In the *u* configuration, highest occupied molecular orbital (HOMO) is described to be the only orbital that can have a significant overlap with the graphene orbital, thus NH_3 acts as an electron donor. However, both HOMO and lowest unoccupied molecular orbital (LUMO) in the *d* configuration interact with the graphene surface, resulting in zero charge transfer. The same group also demonstrated that LUMO of NO_2 is located at 0.3 eV below the Dirac points; therefore NO_2 accepts a large charge from graphene. Yoon *et al.*[58] demonstrated CO_2 sensitivity of the graphene device up to 10–100 ppm for a fast response time of 8–10 sec (Figure 7). CO_2 molecule acts as a donor/acceptor on the graphene sheet. Again, the physical adsorption of CO_2 gas on the graphene sheet is the dominant sensing mechanism that indicates a charge transfer. The recovery time for CO_2 was found shorter than NH_3 and NO_2 due to weaker interaction with graphene.

Chu *et al.*[59] studied hydrogen detection using epitaxial graphene with a thin catalyst layer of Pt, which showed a reduced resistance upon exposing it with 1% hydrogen at various temperatures (Figure 8 *a*). Hydrogen accumulates at the surface of Pt after dissociation and forms a covalent bond with graphene. It is known that hydrogenated graphene has an increased work function, which causes the Fermi-level shift to become larger. Therefore, the free carrier will increase. Chen *et al.*[60] also showed change in graphene conductivity upon exposure of 1.25% oxygen (Figure 8 *b*). Oxygen upon exposure to graphene forms epoxide and carboxylic groups that are electron-withdrawing and increase concentration of holes in the conduction band, which significantly decreases the resistance.

Schedin *et al.*[54] were the first to fabricate microscopic sensor capable of detecting individual gas molecules. Their Hall effect measurements show the generation of extra charge carrier during gas absorption that provided strongest response to the change in charge carrier density near the Dirac point (Figure 8). They have shown that graphene resistivity is sensitive to the adsorption of gases. The change in magnitude and sign of the resistivity was revealed, as an indication of whether the adsorbed gas is an electron acceptor or donor (Figure 9 *a*). In addition, change in Hall conductivity caused by adding one electron demonstrated the ability of graphene to detect single adsorbed molecule (Figure 9 *b*). It is concluded that adsorption of acceptor gas can increase the number of holes or the number of electrons for donor gas. This study claimed that graphene-based gas sensor has a limit of detection as low as parts per billion. Furthermore, to reduce contact resistance, a high driving current was used to reduce the Johnson noise by annealing few layers of graphene. Their optimized sensor could detect single NO_2 molecule. Furthermore, the noise at low frequencies can also be used as a parameter to enhance the selectivity of the graphene-based sensors. The gas molecules during adsorption process can create specific traps and scattering centres in the graphene sheet, resulting in fluctuation in either charge mobility or carrier concentration. The frequency range of the resulting noise and the relative resistance change can provide distinct signature for different gases. Most of the sensors showed poor reversibility,

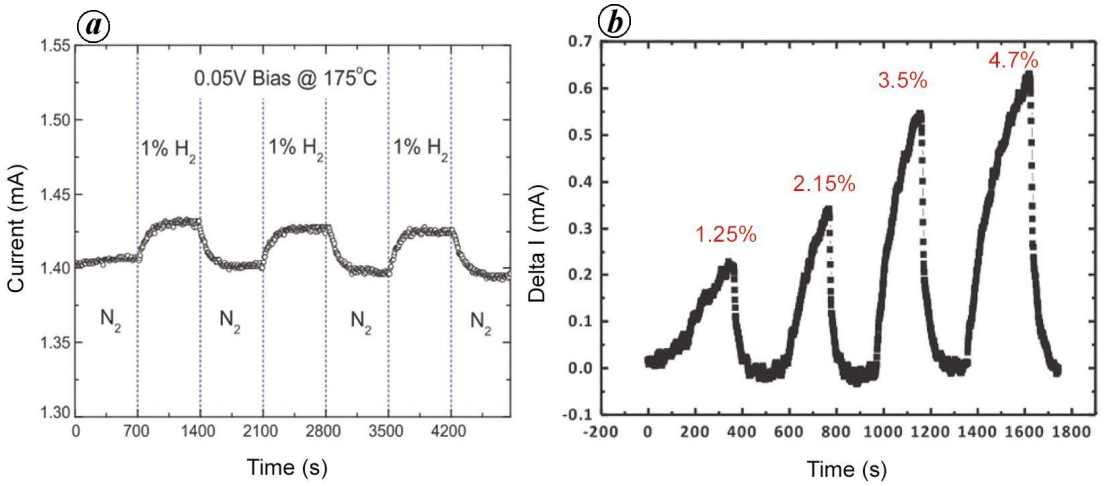

Figure 8. ***a***, Current response of the graphene sensor measured with time of exposure of 1% hydrogen. ***b***, Current change in graphene-based gas sensor to different concentrations of oxygen[59,60].

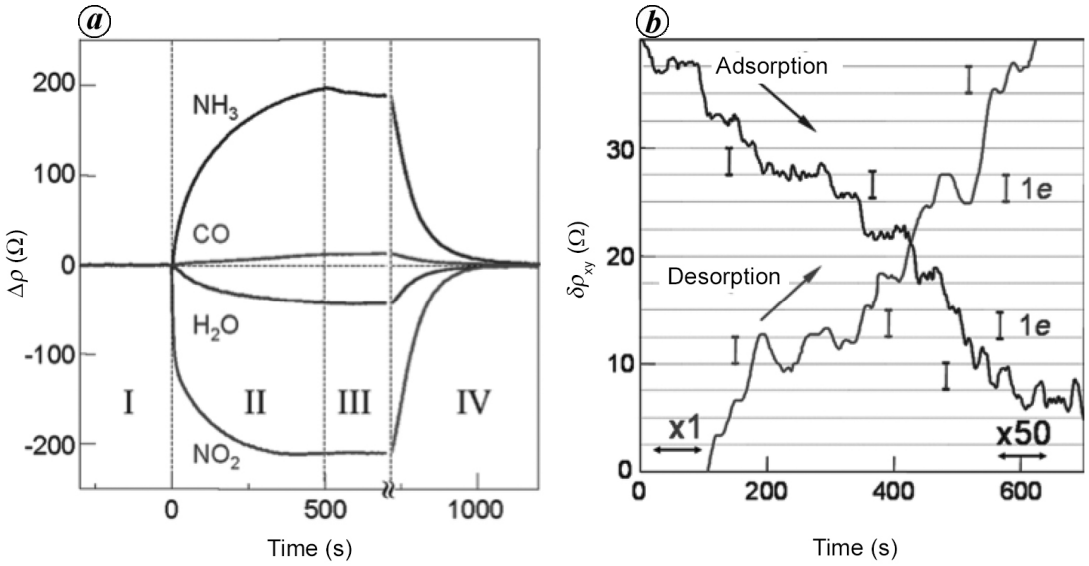

Figure 9. ***a***, Change in resistivity of graphene after exposure to different gases (NH_3, CO, CO_2, NO_2) diluted to 1 ppm concentration. The positive and negative signs are shown to indicate electron and hole doping respectively. ***b***, Change in Hall resistivity near the Dirac point during adsorption of NO_2 and its desorption at 50°C (shown by arrow)[54].

which causes an unreliable sensing output along with lower sensitivity. Ultraviolet light was used to clean the sensing layer adsorbed during chemical exposure[61]. The limit of detection of NO was tested to be 158 ppq, which is three times lower than that achieved using CNT-based sensors. The sensor also showed sensitivity towards other gases, including NH_3, NO_2 and NO, with limit of detection in the range 38.8–136 ppt. Figure 10 *a* and *b* shows the change in conductance of the graphene sensor upon exposure to NH_3 with and without UV exposure respectively. It is clear that the sensitivity of the sensor enhances to ~ 83 ppb to 200 ppt.

The defects in graphene were presented to be playing a significant role in gas sensing. First principle simulations indicated that the defective sites in graphene interact strongly with CO, NO and NO_2, but weakly with NH_3. Nitrogen doping of graphene showed a strong binding with NO_2 molecule, whereas boron doping exhibits enhanced interactions with NO_2, NH_3 and NO gas molecules. Ao *et al.*[34] studied the adsorption of CO on aluminum-doped graphene using density functional theory. CO adsorbs strongly on graphene through Al–CO bonding. However, CO molecules weakly adsorb onto pristine graphene with a small binding energy. Metal oxides have been used for sensing applications due to their large specific surface area and mechanical flexibility. Composites with graphene in their hybrid architectures have shown the possibility to improve their sensing characteristics[62].

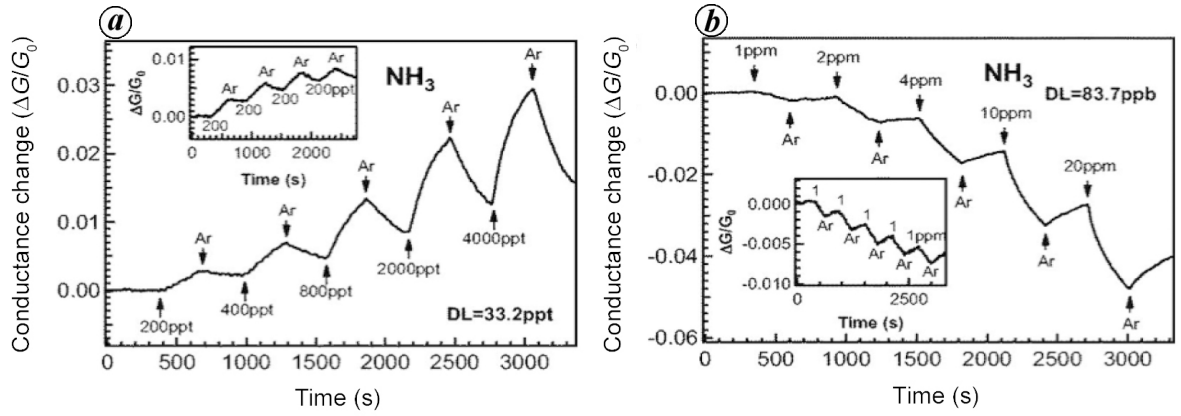

Figure 10. ***a***, Change in conductance response towards exposure of NH_3 under UV light illumination. (Inset) Sensor response at 200 ppt of NH_3 exposure. ***b***, Change in conductance response to NH_3 without UV light illumination[61].

Noble-metal-decorated graphene composites show their prospects for a new type of sensing material with higher sensitivity and selectivity[63,64].

Conclusion and outlook

CNT and graphene offer various advantages over commercially available sensors such as metal oxide sensors, infrared and optical sensors. The sensitivity of bulky and expensive metal oxide sensors is found moderate between 30 and 50 ppm. In addition, these sensors require a high operating temperature up to 600°C, which raises the power consumption, operation complexity and device price. However, CNT and graphene sensors provide high sensitivity up to sub ppb level for a range of gases at room temperature.

CNT have been presented as an ideal material for developing sensor technology because of their unique material characteristics of small size with high aspect ratio that enables them to integrate into large electronic systems. High fraction of surface atoms acts as a highly sensitive detection layer with efficient electron conduction channel. CNT present a broad range of chemical sensitivities for developing sensors for different areas such as industrial, environment, medical and military. Despite their promises, CNT still face considerable challenges due to involved structural heterogeneity. The existing growth methods do not allow controlling structural uniformity such as diameter, number of graphene walls and electrical properties by separating metallic and semiconducting CNT. However, freestanding graphene also presented the possibility of high sensitivity towards detection of chemical analytes, in addition to several advantages over CNT-based sensors. Graphene is shown to exhibit inherently low electrical noise at room temperature and high electron mobility, which enhance its sensitivity compared to CNT. Also, compared to CNT, graphene is relatively easier for electrical manipulation. But there are challenges involved in utilizing graphene as a highly sensitive sensors, which lie in controlling different number of layers, preserving them from folding and bending during processing, minimizing substrate effects, in addition to avoiding undesired surface contamination produced during micro-fabrication processes.

However, recent efforts have succeeded in overcoming the above-mentioned issues, thus increasing their usefulness to achieve multifunctionality of these sensors. In future, the largest potential for developing CNT-based sensor technology lies in the development of compact, low power, portable sensor arrays that should allow detecting and screening multiple chemical analytes. Additionally, room-temperature operation will eliminate the requirement of complex heating parameter, which will result in low power consumption and improve the sensor battery lifetime. Decreased manufacturing cost combined with wireless technology will allow production of large wireless sensor networks. These show prospects towards achieving a sensor material with superior sensitivity, much reduced size, light weight, compact and extended life for innumerable applications.

1. Chen, Z., Appenzeller, J., Knoch, J., Lin, Y. M. and Avouris, P., The role of metal–nanotube contact in the performance of carbon nanotube field-effect transistors. *Nano Lett.*, 2005, **5**, 1497–1502.
2. Dresselhaus, M. S., Dresselhaus, G. and Avouris, P., *Carbon Nanotubes: Synthesis, Structure, Properties and Applications*, Springer, Berlin, 2001, vol. 80.
3. Tans, S. J., Verschueren, A. R. M. and Dekker, C., Room-temperature transistor based on a single carbon nanotube. *Nature*, 1998, **393**, 49–52.
4. Martel, R., Schmidt, T., Shea, H. R., Hertel, T. and Avouris, P., Single- and multi-wall carbon nanotube field-effect transistors. *Appl. Phys. Lett.*, 1998, **73**, 2447–2449.
5. Kong, J., Franklin, N. R., Zhou, C., Chapline, M. G., Peng, S., Cho, K. and Dai, H., Nanotube molecular wires as chemical sensors. *Science*, 2000, **287**, 622–625.
6. Collins, P. G., Bradley, K., Ishigami, M. and Zettl, A., Extreme oxygen sensitivity of electronic properties of carbon nanotubes. *Science*, 2000, **287**, 1801–1804.

7. Balasubramanian, K. and Burghard, M., Chemically functionalized carbon nanotubes. *Small*, 2005, **1**, 180–192.
8. Geim, A. K. and Novoselov, K. S., The rise of graphene. *Nature Mater.*, 2007, **6**, 183–191.
9. Dutta, P. and Horn, P. M., Low-frequency fluctuations in solids –1/*f* noise. *Rev. Mod. Phys*., 1981, **53**, 497–516.
10. Star, A., Gabriel, J. C. P., Bradley, K. and Gruner, G., Electronic detection of specific protein binding using nanotube FET devices. *Nano Lett*., 2003, **3**, 459–463.
11. Hecht, D. S., Hu, L. and Irvin, G., Emerging transparent electrodes based on thin films of carbon nanotubes, graphene, and metallic nanostructures. *Adv. Mater*., 2011, **23**, 1482–1513.
12. Hecht, D. S. and Gruner G., In *Flexible Electronics* (eds Wong, W. and Salleo, A.), Springer, 2009.
13. Hecht, D. S., *Properties and Applications of Carbon Nanotube Films: A Revolutionary Material for Transparent and Flexible Electronics*, VDM-Verlag, 2008.
14. Grüner, G., Carbon nanotube films for transparent and plastic electronics. *J. Mater. Chem*., 2006, **16**, 3533–3539.
15. Artukovic, E., Kaempgen, M., Hecht, D. S., Roth, S. and Grüner, G., Transparent and flexible carbon nanotube transistors. *Nano Lett*., 2005, **5**, 757–760.
16. Star, A., Tu, E., Niemann, J., Gabriel, J. C. P., Joiner, C. S. and Valcke, C., Label-free detection of DNA hybridization using carbon nanotube network field-effect transistors. *Proc. Natl. Acad. Sci. USA*, 2006, **103**, 921–926.
17. Cao, Q. *et al.*, Highly bendable, transparent thin-film transistors that use carbon-nanotube-based conductors and semiconductors with elastomeric dielectrics. *Adv. Mater*., 2006, **18**, 304–309.
18. Hu, L., Hecht, D. S. and Gruner, G., Percolation in transparent and conducting carbon nanotube networks. *Nano Lett*., 2004, **4**, 2513–2517.
19. Zhang, T., Mubeen, S., Myung, N. V. and Deshusses, M. A., Recent progress in carbon nanotube-based gas sensors. *Nanotechnology*, 2008, **19**, 332001.
20. Ijima, S., Helical microtubules of graphic cabon. *Nature*, 1991, **354**, 56–58.
21. An, K. H., Jeong, S. Y., Hwang, H. R. and Lee, Y. H., Enhanced sensitivity of a gas sensor incorporating single-walled carbon nanotube–polypyrrole nanocomposites. *Adv. Mater*., 2004, **16**, 1005–1009.
22. Dai, L. M., Soundarrajan, P. and Kim, T., Sensors and sensor arrays based on conjugated polymers and carbon nanotubes. *Appl. Chem.*, 2002, **74**, 1753–1772.
23. Bai, H. and Shi, G. Q., Gas sensors based on conducting polymers. *Sensors*, 2007, **7**, 267–307.
24. Wei, C., Dai, L. M., Roy, A. and Tolle, T. B., Multifunctional chemical vapor sensors of aligned carbon nanotube and polymer composites. *J. Am. Chem. Soc.*, 2006, **128**, 1412–1413.
25. Kong, J., Chapline, M. G. and Dai, H. J., Functionalized carbon nanotubes for molecular hydrogen sensors. *Adv. Mater*., 2001, **13**, 1384–1386.
26. Fam, D. W. H., Tok, A. I. Y., Palaniappan, A., Nopphawan, P., Lohani, A. and Mhaisalkar, S. G., Selective sensing of hydrogen sulphide using silver nanoparticle decorated carbon nanotubes. *Sensors Actuators B*, 2009, **138**, 189–192.
27. Star, A., Joshi, V., Skarupo, S., Thomas, D. and Gabriel, J. C. P., Gas sensor array based on metal-decorated carbon nanotubes. *J. Phys. Chem. B*, 2006, **110**, 21014–21020.
28. Du, N., Zhang, H., Chen, B. D., Ma, X. Y., Liu, Z. H., Wu, J. B. and Yang, D. R., Porous indium oxide nanotubes: layer-by-layer assembly on carbon–nanotube templates and application for room-temperature NH_3 gas sensors. *Adv. Mater*., 2007, **19**, 1641–1645.
29. Zhao, W. *et al*., A carbon monoxide gas sensor using oxygen plasma modified carbon nanotubes. *Nanotechnology*, 2012, **23**, 425502–425508.
30. Dong, K.-Y. *et al.*, Detection of a CO and NH_3 gas mixture using carboxylic acid-functionalized single-walled carbon nanotubes. *Nanoscale Res. Lett.*, 2013, **8**, 12.
31. Ong, K. G. and Grimes, C. A., A carbon nanotube-based sensor for CO_2 monitoring. *Sensors*, 2001, **1**, 193–205.
32. Kauffman, D. R. and Star, A., Chemically induced potential barriers at the carbon nanotube−metal nanoparticle interface. *Nano Lett.*, 2007, **7**, 1863–1868.
33. Vedala, H., Sorescu, D. C., Kotchey, G. P. and Star, A., Chemical sensitivity of graphene edges decorated with metal nanoparticles. *Nano Lett*., 2011, **11**, 2342–2347.
34. Ao, Z. M., Yang, J., Li, S. and Jiang, Q., Enhancement of CO detection in Al doped graphene. *Chem. Phys. Lett.*, 2008, **461**, 276–279.
35. Kumar, M. K. and Ramaprabhu, S., Nanostructured Pt functionlized multiwalled carbon nanotube based hydrogen sensor. *J. Phys. Chem. B*, 2006, **110**, 11291–11298.
36. Staii, C., Johnson, A. T., Chmn, M. and Gelperin, A., DNA-decorated carbon nanotubes for chemical sensing. *Nano Lett*., 2005, **5**, 1774–1778.
37. Star, A. and Kauffman, D. R., Carbon nanotube gas and vapor sensors. *Angew. Chem. Int. Ed*., 2008, **47**, 6550–6570.
38. Nguyen, L. Q., Phan, P. Q., Duong, H. N., Nguyen, C. D. and Nguyen, L. H., Enhancement of NH_3 gas sensitivity at room temperature by carbon nanotube-based sensor coated with CO nanoparticles. *Sensors*, 2013, **13**, 1754–1762.
39. Lee, J.-H., Kim, J., Seo, H. W., Song, J.-W., Lee, E.-S. and Won, M., Large-scale integrated carbon nanotube gas sensors. *Sensors Actuators B*, 2008, **129**, 628–631.
40. Chang-Soo Han, Jeong, H. Y., Lee, D., Choi, H. K., Lee, D. H. and Kim, J., Flexible room-temperature NO_2 gas sensors based on carbon nanotubes/reduced graphene hybrid films. *Appl. Phys. Lett*., 2010, **96**, 213105–213107.
41. Chen, G., Paronyan, T. M., Pigos, E. M. and Harutyunyan, A. R., Enhanced gas sensing in pristine carbon nanotubes under continuous ultraviolet light illumination. *Sci. Rep*., 2012, **2**, 343; doi: 10.1038/srep00343.
42. Zhang, X., Yang, B., Wang, X. and Luo, C., Effect of plasma treatment on multi-walled carbon nanotubes for the detection of H_2S and SO_2. *Sensors*, 2012, **12**, 9375–9385.
43. Varghese, O. K., Kichambare, P. D., Gong, D., Ong, K. G., Dickey, E. C. and Grimes, C. A., Gas sensing characteristics of multi-wall carbon nanotubes. *Sensors Actuators B*, 2001, **81**, 32–41.
44. Chopra, S., McGuire, K., Gothard, N., Rao, A. M. and Pham, A., Selective gas detection using a carbon nanotube sensor. *Appl. Phys. Lett*., 2003, **83**, 2280–2282.
45. Zhao, J., Buldum, A., Han, J. and Lu, J. P., Gas molecule adsorption in carbon nanotubes and nanotube bundles. *Nanotechnology*, 2002, **13**, 195–200.
46. Pumera, P., Ambrosi, A., Bonanni, A., Chang, E. L. K. and Poh, H. L., Graphene for electrochemical sensing and biosensing. *Trends Anal. Chem*., 2010, **29**, 954–965.
47. Hill, E. W., Vijayaragahvan, A. and Novoselov, K., Graphene sensors. *IEEE Sensors J*., 2011, **11**, 3161–3170.
48. Bunch, J. S. *et al.*, Electromechanical resonators from graphene sheets. *Science*, 2007, **315**, 490–493.
49. Lemme, M. C., Echtermeyer, T. J., Bus, M. and Kurz, H., A graphene field-effect device. *IEEE Electron Device Lett*., 2007, **28**, 282–284.
50. Williams, J. R., Dicarlo, L. and Marcus, C. M., Quantum hall effect in a gate-controlled *p–n* junction of graphene. *Science*, 2007, **317**, 638–641.
51. Satndley, B., Bao, W., Zhang, H., Bruck, J., Lau, C. N. and Bockrath, M., Graphene-based atomic-scale switches. *Nano Lett.*, 2008, **8**, 3345–3349.
52. Stoller, M. D., Park, S., Bhu, Y., An, J. and Ruoff, R., Graphene-based ultracapacitors. *Nano Lett*., 2008, **8**, 3498–3502.

53. Stampfer, C., Schurtenberger, E., Molitor, F., Guttinger, J., Ihn, T. and Ensslin, K., Tunable graphene single electron transistor. *Nano Lett*., 2008, **8**, 2378–2383.
54. Schedin, F., Geim, A. K., Morozov, S. V., Hil, E. W., Blake, P., Katsnelson, M. I. and Novoselov, K. S., Detection of individual gas molecules adsorbed on graphene. *Nature Mater*., 2007, **6**, 652–655.
55. Wang, X., Zhi, L. and Muellen, K., Transparent, conductive graphene electrodes for dye-sensitized solar cells. *Nano Lett*., 2008, **8**, 323–327.
56. Romero, H. E., Joshi, P., Gupta, A. K., Gutierrez, H. R., Cole, M. W., Tadigadapa, S. A. and Eklund, O. C., Adsorption of ammonia on graphene. *Nanotechnology*, 2009, **20**, 245501–245508.
57. Leenaerts, O., Partoens, B. and Peeters, F. M., Adsorption of small molecules on graphene. *Microelectron. J.*, 2009, **40**, 860–862.
58. Yoon, H. J., Jun, D. H., Yang, J. H., Zhou, Z., Yang, S. S. and Cheng, M. M., Carbon dioxide gas sensor using a graphene sheet. *Sensors Actuators B*, 2011, **157**, 310–313.
59. Chu, B. H. *et al.*, Hydrogen detection using platinum coated graphene grown on SiC. *Sensors Actuators B*, 2011, **157**, 500–503.
60. Chen, C. W. *et al.*, Oxygen sensors made by monolayer graphene under room temperature. *Appl. Phys. Lett*., 2011, **99**, 243502.
61. Chen, G., Paronyan, T. M. and Harutyunyan, A. R., Sub-ppt gas detection with pristine graphene. *Appl. Phys. Lett*., 2012, **101**, 053119–053122.
62. Yi, J., Lee, J. M. and Park, W., Vertically aligned ZnO nanorods and graphene hybrid architectures for high-sensitive flexible gas sensors. *Sensors Actuators B*, 2012, **155**, 264–269.
63. Yin, P. T., Kim, T.-H., Choic, J.-W. and Lee, K.-B., Prospects for graphene–nanoparticle-based hybrid sensors. *Phys. Chem. Chem. Phys*., 2013, **15**, 12785–12799.
64. Gutés, A., Hsia, B., Sussman, A., Mickelson, W., Zettl, A., Carraro, C. and Maboudian, R., Graphene decoration with metal nanoparticles: Towards easy integration for sensing applications. *Nanoscale*, 2012, **4**, 438–440.